Tuijin Jishu/Journal of Propulsion Technology
ISSN: 1001-4055
Vol. 45 No. 4 (2024)

Investigations on Tensile and Flexural Behavior of Delaminated E-Glass/Epoxy, Carbon/Epoxy and E-Glass/Carbon/Epoxy Composites Using Hybrid Teaching Learning-Based Optimization

Phaneendra Kumar Kopparthi[1], Kiran Kumar Yadav Aerra[2,*], Bhaskara Rao Pathakokila[1] and Suresh Gamini[2]

[1]Department *of Mechanical Engineering, Vignan's Lara Institute of Technology & Science, Vadlamudi, Andhra Pradesh, India, PIN. 522 213*

[2]*Department of Mechanical Engineering, Vignan's Foundation for Science, Technology & Research, Vadlamudi, Andhra Pradesh, India, PIN. 522 213*

** Corresponding Author*

Kiran Kumar Yadav Aerra

Department of Mechanical Engineering

Vignan's Foundation for Science, Technology & Research, *Vadlamudi, Andhra Pradesh, India, PIN 522 213*

Abstract

The defects in the fiber reinforced polymer composites may occurs during the production process and/or due to low velocity impact. These defects initiate a more crucial damage form such as delamination. The delamination is a common failure and which destroys the structural integrity of composites. Hence, to study the influence of induced delamination on tensile and flexural performance of E-glass/epoxy, carbon/epoxy and carbon/E-glass/epoxy composites, the laminates were manufactured with constant fiber volume fraction inserting an artificial defect (polytetrafluoroethylene) at the preferred interface. Artificial defects with circular and square shapes were used in the present study to have a controlled defect size and form. The location of artificial defect in E-glass/epoxy and carbon/epoxy composites did not affect their tensile strengths considerably whereas the tensile strength of hybrid composite was affected. Moreover, the flexural properties of delaminated composites were affected by both the defect shape and its location in thickness direction due to variation in bonding strength in thickness direction. Thus, a hybrid teaching learning-based optimization (HTLBO) was implemented to suggest a delaminated composite with optimal control parameters (location of defect, area of defect and density of composite) for minimization of tensile and flexural strengths. The experimental results were compared with those of HTLBO and they agreed within 4% error.

Keywords Tensile strength · flexural strength · artificial defect · delamination · hybrid teaching learning-based optimization

1. Introduction

Composite is a structural material derived from two or more constituents having dissimilar physical, chemical, and mechanical properties. Composites can be developed to satisfy specific geometrical, structural and mechanical requirements depending upon their application. The composites possess high strength to weight and stiffness to weight ratios. Moreover, they are highly resistant to corrosion along with offering good fatigue resistance.

Automobile, aeronautical and marine industries are the typical applications demanding fiber reinforced polymer (FRP) composites for structural components [1]. However, the parts of a structure in the real situation may experience defects due to impact and during production process. The existence of defects leads to induce delamination [2]. Delamination is a crucial failure which highly deteriorates the structural integrity of the composite. As a result, the strength and stiffness in the thickness direction drastically vary. For this reason, investigating the flexural performance of FRP composites with induced delaminations is a major concern to the researchers.

Gabor and Viktor [3] investigated the tensile and compressive behaviors of carbon/epoxy and glass/epoxy composites embedded with square and circular shape defects. The longitudinal strains increased substantially in the delaminated zone for samples under tension. In the specimens subjected to compression, the absolute transverse strains in delaminated zone increased much higher than that of the intact zone. Aslan et al. [4] conducted similar studies on the tensile, compressive and flexural behaviours of E-glass/epoxy composites containing multiple strip type, circular and peanut shaped delaminations. Their existence affected compressive and flexural strengths much higher than the tensile strength. Reis et al. [5] focused on the tensile behavior of carbon/epoxy laminates due to the existence of strip delamination. The presence of embedded delaminations decreased the tensile strength. Importantly, the size of delamination did not affect the static tensile strength. The matrix damage, fiber fracture and fiber-matrix debonding appeared as the predominant modes of failure. Ashir et al. [6] investigated the effect of defect position on the mechanical properties of carbon/epoxy laminates. The tensile strength decreased exponentially with respect to increase in distance of defect position from top surface. Amaro et al. [7] presented three-point bending behavior of carbon/epoxy composite with single strip delamination. The delamination considerably decreased both strength and modulus. Liu et al. [8] studied the flexural performance of carbon/epoxy composites with delamination existing at different interfaces. The failure modes like in-ply and interlaminar modes were predominant in all laminates. The existence of pre-delamination and its location affected the size of damage and flexural properties. Pradeep et al. [9] documented the variation in the flexural properties of glass/epoxy composites containing embedded circular delaminations of different sizes at selected locations. The flexural strength was higher for the composite containing defect at mid-plane. It was lower for the composite consisting of defect below the first ply on compression side. Kopparthi et al. [10] presented the effect of circular and square delaminations on the flexural properties of glass/epoxy composites subjected to three-point loading. The flexural strengths and modulii of composites with embedded defect of same shape and size decreased with respect to its distance from top surface. Kopparthi et al. [11] also investigated the effect of single circular delamination on the flexural response of a multilayer carbon/epoxy composite under pure bending. The existence of delamination decreased bending strength and stiffness. Moreover, local out of plane displacement occurred due to local buckling.

Optimization is one of the most important techniques of the modern era associated with engineering designs in certain advanced fields such as aeronautics and automotive industries. Normally, weight reduction, use of less expensive materials and improved strength has been pursued in the design of various mechanical systems. Several optimization experiments on composite structures can be performed from two perspectives. The first perspective is concerned with the process of optimization, which includes different types of optimization problems and algorithms. The quantity and quality of objective functions, as well as design variables are analyzed from this perspective. Algorithms for various types of optimization problems define the process of optimizing design variables in order to accomplish goal functions. In the next perspective, the types of composite structures, objective functions, design variables, and constraints are examined. By probing these two areas separately and integrating them comprehensively, a great deal of insight into composite structure optimization can be gained. The teaching learning-based optimization (TLBO) is a powerful and one of the best methods for optimizing the mechanical properties of composites and the process parameters in manufacturing industries [12, 13]. It has been observed that the TLBO appears more successful in contrast to genetic algorithm (GA) in the context of experimental research focused on machining of FRP composites [14, 15]. TLBO needs a non-linear regression model as a function of variables which affect the objective function to develop the new variables to forecast the knowledge transfer from the teacher to the learners and as well as the interaction among the learners [16].

Although TLBO was designed for continuous issues, it must be modified when applied to discrete problems. TLBO has the tendency to get fixed in local optima when solving real-world problems. Hence, the researchers have been working to develop acceptable coding and decoding strategies for TLBO and improve the algorithm's exploitation potential. In the present study, the authors have introduced a hybrid teaching learning-based optimization (HTLBO) to enhance the performance of basic TLBO [17]. HTLBO uses a variety of teaching methodologies to teach the learners at each level of hierarchy. The learners at each level receive instruction from a variety of teachers. Accordingly, the exploitation and exploration trends are balanced. Similarly, the original learning technique is refined throughout the learning phase. As a result, each learner not only learns from a superior but also from a worse one with the objective of using the population's information and improving total knowledge levels fully. Additionally, the entire population is divided into two groups such as teaching-learning and self-learning. There are three categories of teaching-learning namely good, average and poor. Prior to the iterative procedure, all individuals' hierarchies are dynamically modified based on their objective function values. This competitive mechanism ensures the population's vitality and long-term viability. The implementation of aforementioned tactics may lead to improvement of HTLBO's overall performance [18]. The HTLBO is a global search strategy to identify the optimal sequence of operations quickly under various feasibility constraints consideration [19]. In the literature, various population-based metaheuristic hybrid schemes such as optimal stopping rule (OSR)-genetic algorithm (GA), OSR-TLBO and OSR-firefly algorithm (FA) are suggested as hybrid methodologies. These algorithms have a rapid convergence rate and take less time to implement [20]. Very few researchers employed hybrid methodologies to the problems of composite industry such as grey-based Taguchi method [21], response surface methodology (RSM)-grey relational analysis (GRA)-TLBO [22] and GRA integrated TLBO for optimizing the fabrication parameters, machining indicators and wear parameters respectively.

The hybridization of stiffer fibers such as carbon fibers with more yielding glass fibers increases the impact properties and strain to failure of the composite. Additionally, the inclusion of glass fibers improves the fatigue properties of the hybrid composite [23] due to its increased stiffness. This can be attributed to high stiffened carbon fibers. The hybrid composites are used in commercial, industrial, aerospace and marine primary structures. Specifically, they have extensive collection of benefits in the aerospace industry such as great fatigue life, corrosion resistance and impact resistance. Although the hybrid composites have the greater control of these properties, their strength and stiffness properties are greatly influenced due to the cracks initiated under low velocity impact and during the service life. Subsequently, their existence at the ply interfaces leads to separation of adjacent plies. For this reason, the investigation of mechanical performance of a hybrid composite containing a separation at the interface is needed. To accomplish this study, a delaminated hybrid (E-glass/carbon/epoxy) composite with two extreme carbon fiber plies on both sides with eight glass fiber plies at the middle was considered for optimum combination for good balance between the properties [24, 25]. The delamination was created inserting a circular or square defect in the composite at the selected ply interface during manufacturing. The tensile and flexural tests were conducted to know the effect of defect existence on tensile and flexural strengths of hybrid composite. These results were compared with those of E-glass/epoxy and carbon/epoxy composites. A hybrid teaching learning-based optimization was implemented to identify the optimal variables (area of defect, location and composite material density) for minimization of tensile and flexural strengths.

2. Material and Methods

2.1 Fabrication of composite laminates

E-glass/epoxy, carbon/epoxy and hybrid (E-glass/carbon/epoxy) composite laminates were manufactured with 12 layers of woven fabric (each 0.18 mm thickness) by hand layup method to 370 mm × 350 mm × 2.1 mm size at room temperature to conduct the present experiments. A mixture of epoxy (Lapox L12) and hardener (K6) was used as matrix material. The hybrid laminate contained 4 layers of carbon fabric (2 layers at the top and 2 layers at the bottom). And, the remaining 8 layers were E-glass. The composites with induced delamination were produced inserting a single polytetrafluoroethylene (PTFE) film of 80 μm thickness at the selected position in the specimen center during hand layup. The presence of a PTFE (polytetrafluoroethylene) film in a laminate will act as a "defect" since it has the potential to impair the structural integrity and performance of the composite material.

The inclusion of PTFE film in the composite structure is atypical and intended, as its presence might cause an artificial disturbance in the material. More precisely, the addition of a PTFE layer introduces an external substance that may not possess the same mechanical properties or bonding characteristics as the main composite materials, such as E-glass/epoxy, carbon/epoxy, or other combinations. The lack of consistency can cause differences in rigidity, durability, and bonding, which can subsequently lead to concentrated stress, separation, and diminished overall mechanical effectiveness. Furthermore, the incorporation of PTFE film serves as a deliberate and regulated experimental method in our research to replicate any defects that might arise either from the production process or as a result of low-velocity impacts. This methodology enables us to methodically examine the reaction of the laminate to such disturbances and, eventually, assess the efficacy of our recommended strategies for minimising or optimising the influence of these "defects.". PTFEs with two different shapes (circle and square) were used. The main objective of the present work is to examine the impact of induced delamination, characterised by the existence of square and circular films, on the tensile and flexural properties of composite laminates. The purpose of these artificial disruptions is to replicate actual defects seen in the real world, and our research seeks to evaluate their influence on mechanical characteristics. Square films are employed to replicate flaws characterised by distinct corners and perpendicular angles, which may arise from diverse production procedures or damage sources. It aids in evaluating the impact of these faults on the mechanical characteristics of the composite laminate. Circular defects belong to a distinct category of disruptions that frequently result from various reasons. These faults do not have the sharp corners that square defects have and are more consistently shaped. Our objective is to analyse the influence of circular films on the performance of the composite in order to have a better understanding of the effects of such defects. The size (diameter/side) of PTFE was 8 mm. L1 indicates the location of PTFE film between first and second layers as seen in Figure 1(a).

Figure 1(b) shows the location (L2) of PTFE between fifth and sixth layers. Based on the shape and position of defect in the test sample, the E-glass/epoxy, carbon/epoxy and hybrid (E-glass/carbon/epoxy) composite laminate samples were grouped as described in Table 1. The sizes of tensile and bending test samples confirmed to 250 mm × 25 mm × 2.1 mm and 100 mm × 15 mm × 2.1 mm as per ASTM D3039 [26] and ASTM D790-03 [27] respectively.

(a)

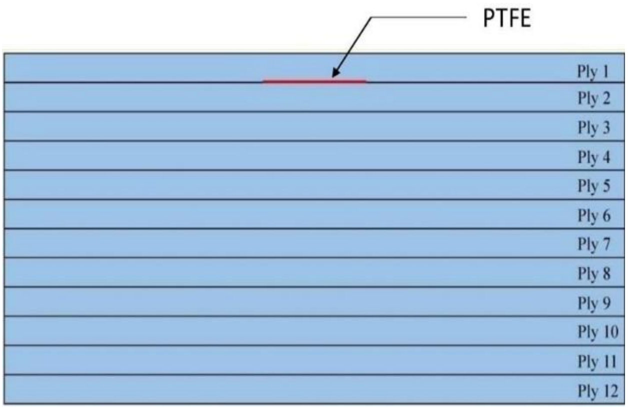

(b)

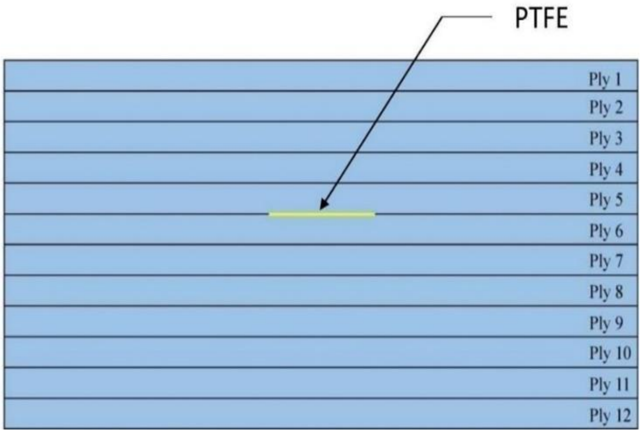

Fig. 1 - Specimens containing single PTFE at (a) L1 and (b) L2 positions

Table 1 - Types of delaminated composites, defect shape and its location

Laminate	Specimen type	Defect shape	Location of PTFE
E-glass/epoxy	GE1	Circle	L1
	GE2	Circle	L2
	GE3	Square	L1
	GE4	Square	L2
Hybrid	GCE1	Circle	L1
	GCE2	Circle	L2
	GCE3	Square	L1
	GCE4	Square	L2
Carbon/epoxy	CE1	Circle	L1
	CE2	Circle	L2
	CE3	Square	L1
	CE4	Square	L2

2.1 Static tensile and flexural tests

Tests were performed on a servo hydraulically operated 40 kN universal testing machine (Figure 2) in displacement control mode to determine tensile and flexural strengths of delaminated E-glass/epoxy, carbon/epoxy and hybrid (E-glass/carbon/epoxy) samples at room temperature. In each case, five samples were tested to determine the strength. The cross-head speed was 2 mm/min. The tensile strength (σ_t) was determined based on the cross-sectional area of gauge length using Eq (1).

$$\sigma_t = \frac{P}{A} \quad (1)$$

In the above, P Maximum load in the load displacement curve

A Cross sectional area in the portion of gauge length

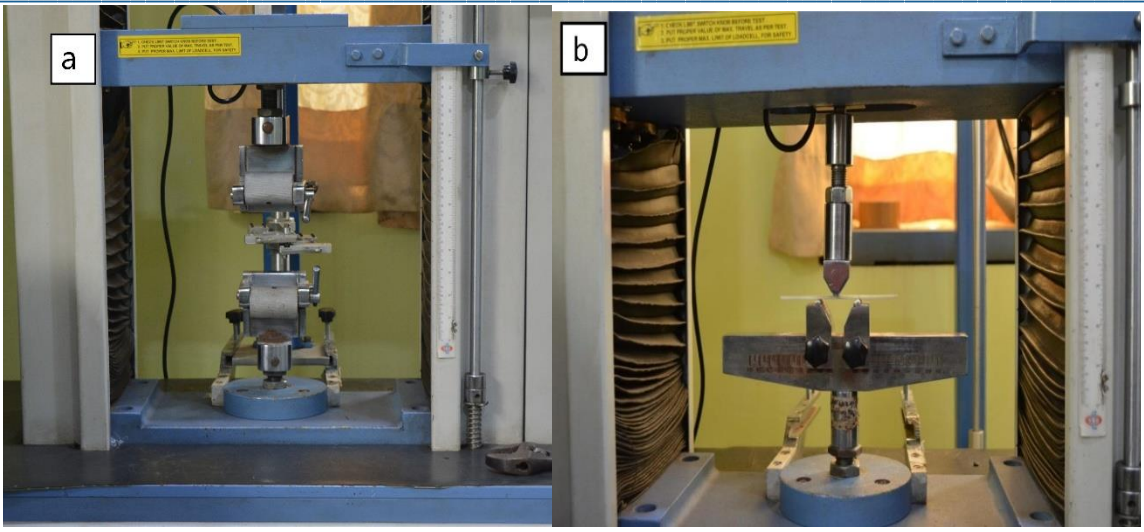

Fig. 2 - Universal testing machine (a) specimen under tension and (b) specimen under bending

The bending tests were performed in three-point loading mode. The recommended span to depth ratio of specimen was 16:1 [27]. The flexural strength (σ_f) was calculated from Eq (2).

$$\sigma_f = \frac{3P_{max}L}{2bd^2} \quad (2)$$

Where, P_{max} maximum bending load

L support span

b beam width

d beam depth

m slope of load deflection curve in elastic portion

3. Optimization

3.1 Teaching learning based optimization

Optimization of a single objective function can be done easily by implementing a traditional gradient-based optimization methodology. But, when it comes to optimization of multiple objective functions, there lies the problem in finding out the best set of solutions simultaneously from a variety of conflicting objectives. Therefore, the optimization of different contradicting objective functions is a challenging phenomenon. The TLBO is such an algorithm used to optimize the learning progress when multiple objectives exist. In the present work, TLBO is implemented in order to minimize the tensile and flexural strengths of delaminated E-glass/epoxy, carbon/epoxy and hybrid (E-glass/carbon/epoxy) composites. The TLBO method has teaching and learning phases. The teaching phase is very similar to a classroom scenario. Aim of the teacher is to improve the overall result of the class in all subjects taught. The teacher identifies fast learners and motivates fast learners to transfer their knowledge to the slow learners through interaction. This methodology improves the overall results. On the other hand, HTLBO (Grey relation analysis integrated with TLBO) is implemented in the current study. The process of implementation of HTLBO is presented in Figure 3.

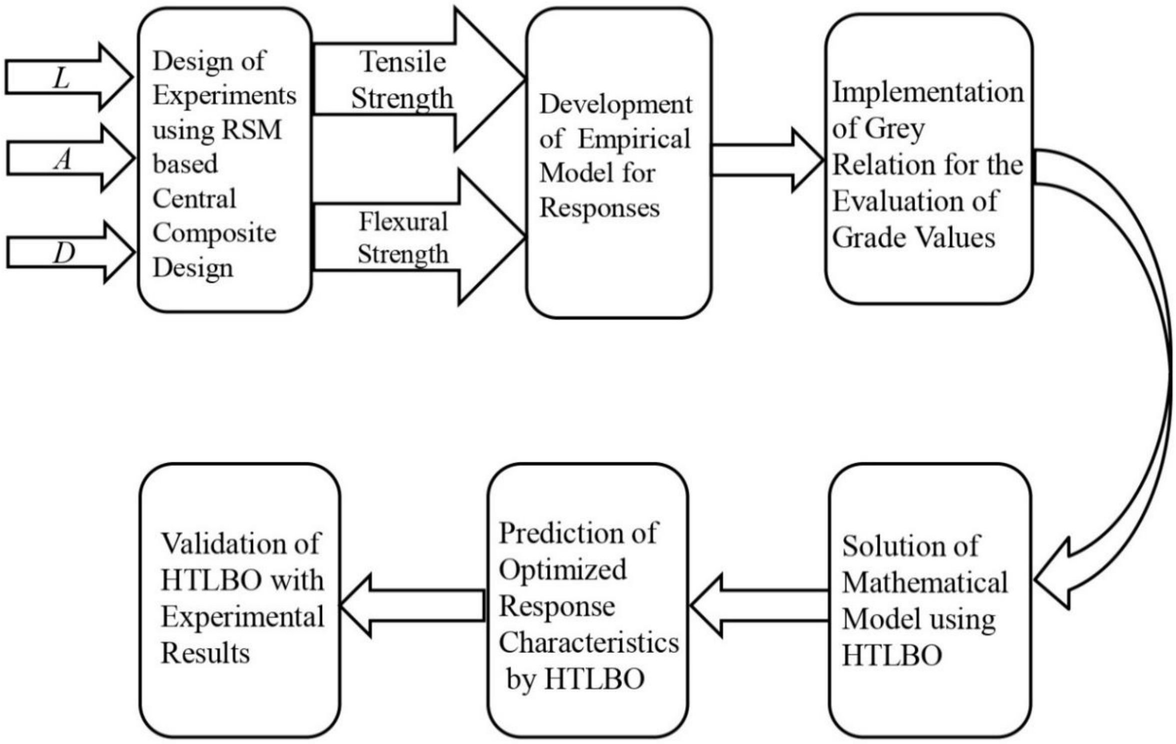

Fig. 3 - Process flow diagram of HTLBO

Table 2 - Designed experiments

Specimen type	L (mm)	A (mm^2)	D (gm/mm^3)
GE1	0.18	50.256	1.9314
GE2	0.9	50.256	1.9314
GE3	0.18	64	1.9314
GE4	0.9	64	1.9314
GCE1	0.18	50.256	2.116
GCE2	0.9	50.256	2.116
GCE3	0.18	64	2.116
GCE4	0.9	64	2.116
CE1	0.18	50.256	1.4968
CE2	0.9	50.256	1.4968
CE3	0.18	64	1.4968
CE4	0.9	64	1.4968

Depending upon RSM based central composite design (CCD), design of twelve experiments considering the location of defect from top surface (L), area of defect (A) and density of laminate (D) as the input variables and tensile strength (σ_t) and flexural strength (σ_f) of delaminated E-glass/epoxy, carbon/epoxy and hybrid (E-glass/carbon/epoxy) composites as responses is presented in Table 2. Empirical models for the responses were generated using RSM. Grey relation grade (GRG) was calculated based on the signal to noise (S/N) ratios, normalization of S/N ratios, deviation sequence and grey relational co-efficient. These mathematical models were used in HTLBO to determine the new values in transfer of their knowledge based on GRG and the ranks are allotted. The optimal parameters (*L*, *A* and *D*) were predicted for minimization of responses (σ_t and σ_f). The final solutions obtained were validated with the experimental results.

The optimal control parameters were determined using GRG. For the two responses, S/N ratios were estimated using smaller the better characteristic Equation [28]. The sequential procedure of determining GRG is presented below.

Step 1: Identification of input parameters and responses

Step 2: Calculation of S/N ratios for the responses

$$\frac{S}{N} = -10\log\left(\left(\frac{1}{n}\right)\left(\sum y^2\right)\right) \quad (3)$$

Where, y^2 variance of y

N number of observations

Step 3: Normalization of S/N ratios

$$x_i(k) = \frac{max\ y_i(k) - y_i(k)}{max\ y_i(k) - min\ y_i(k)} \quad (4)$$

where, $x_i(k)$ response value after normalization

min $y_i(k)$ smallest value among the normalized responses

max $y_i(k)$ largest value among the normalized responses.

Step 4: Determination of deviation sequence

$$\Delta_{0i}(k) = \|x_0(k) - x_i(k)\| \quad (5)$$

Step 5: Determination of GRC

$$\xi_i(k) = \frac{\Delta_{min} + \lambda\Delta_{max}}{\Delta_{0i}(k) + \lambda\Delta_{max}} \quad (6)$$

In the above, λ distinguishing coefficient, $0 \le \lambda \le 1$ ($\lambda = 0.5$ is formal)

Δ_{min} smallest value of Δ_{0i}

Δ_{max} largest value of Δ_{0i}

Step 6: Calculation of GRG

$$\gamma_i = \frac{1}{n}\sum_{k=i}^{n} \xi_i\,(k) \quad (7)$$

Step 7: Allocation of ranks based on GRG

Step 8: Identifying the optimal values based on the rank

4. Results and Discussion

4.1 Tensile and flexural strengths

The tensile and flexural strengths of delaminated E-glass/epoxy, carbon/epoxy and hybrid (E-glass/carbon/epoxy) composites containing single circular and square defects at the preferred positions are given in Table 3. Figures 4 and 5 show the production of load displacement curves using the tensile and bending tests data. The failure of composite under tension was catastrophic with audible sound which indicates the complete breakage of fibers and matrix material. The tensile fracture occurred at the section almost normal to the loading axis.

Table 3 - Tensile and flexural properties of delaminated composites

Composite	Specimen	PTFE location	Tensile strength (MPa)	Standard deviation	Bending strength (MPa)	Standard deviation
E-glass/epoxy	GE1	L1	52.45	4.26	201.76	6.48
	GE2	L2	50.48	3.84	170.81	4.98
	GE3	L1	47.38	2.71	149.88	3.59
	GE4	L2	44.43	3.52	137.33	5.21
	GCE1	L1	84.39	3.69	592.78	1.96
	GCE2	L2	70.98	4.02	536.68	1.36
	GCE3	L1	63.99	5.28	507.38	2.07
	GCE4	L2	53.91	6.81	428.68	2.15
Carbon/epoxy	CE1	L1	307.27	3.64	934.82	2.36
	CE2	L2	305.08	4.62	794.41	3.95
	CE3	L1	299.51	5.61	697.45	2.25
	CE4	L2	291.09	6.14	634.74	5.29

The location of PTFE with similar shape and size in E-glass/epoxy and carbon/epoxy composites does not affect their tensile strengths significantly. But, their tensile stiffnesses are affected considerably along with the stiffness of hybrid composite as evident from the slopes of curves in Figure 4 and whereas for hybrid composite, the tensile strength is affected. Because, two different reinforcements are combined with a common matrix, higher stiffness and tensile strength of the carbon fiber might be the probable reason for increased strength of the hybrid composite. Furthermore, the defect shape also does not affect the tensile strength considerably. In each case, the flexural properties (strength and stiffness) decreased for the laminates containing same circular or square PTFE existing at different depths from top surface due to structural destruction in thickness direction. However, the flexural strength of laminate embedded with single circular PTFE is higher than that of laminate containing square PTFE existing at same depth from top surface due to less stress concentration (Figure 5).

(a)

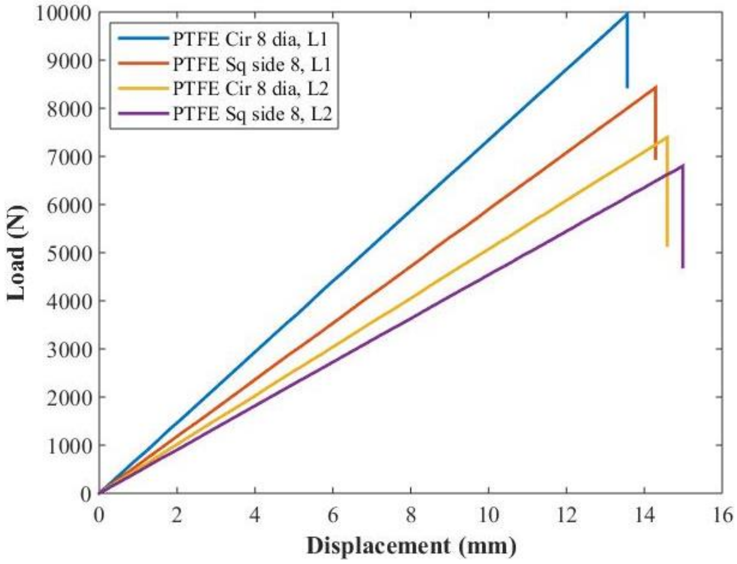

(b)

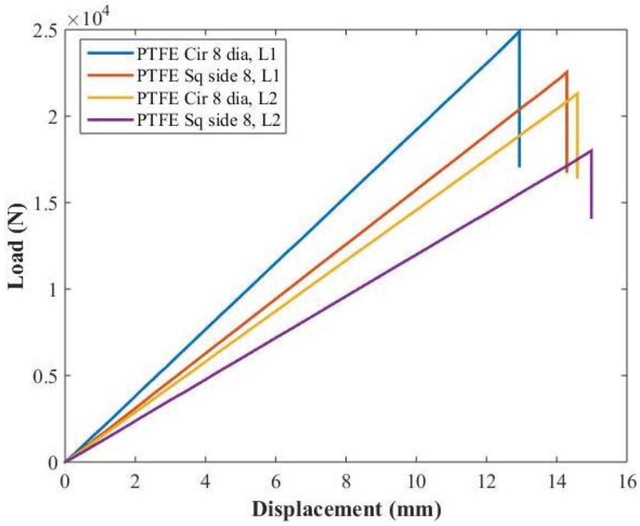

(c)

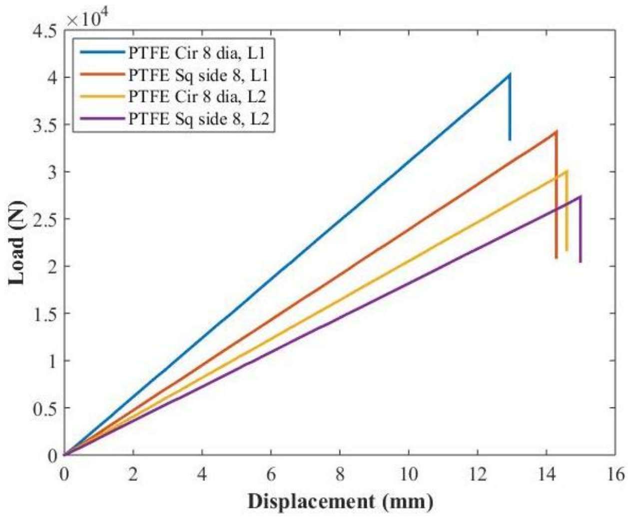

Fig. 4 - Tensile load-displacement plots of (a) E-glass/epoxy, (b) hybrid and (c) carbon/epoxy composites

(a)

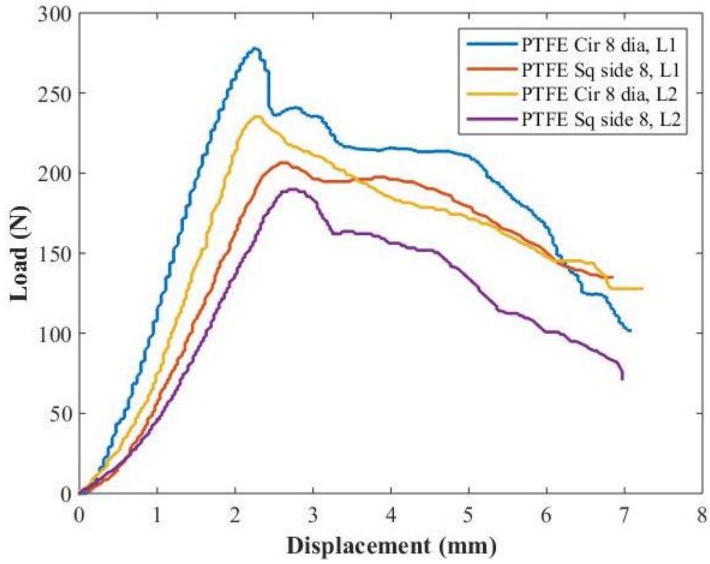
PTFE Cir 8 dia, L1
PTFE Sq side 8, L1
PTFE Cir 8 dia, L2
PTFE Sq side 8, L2
Load (N)
Displacement (mm)

(b)

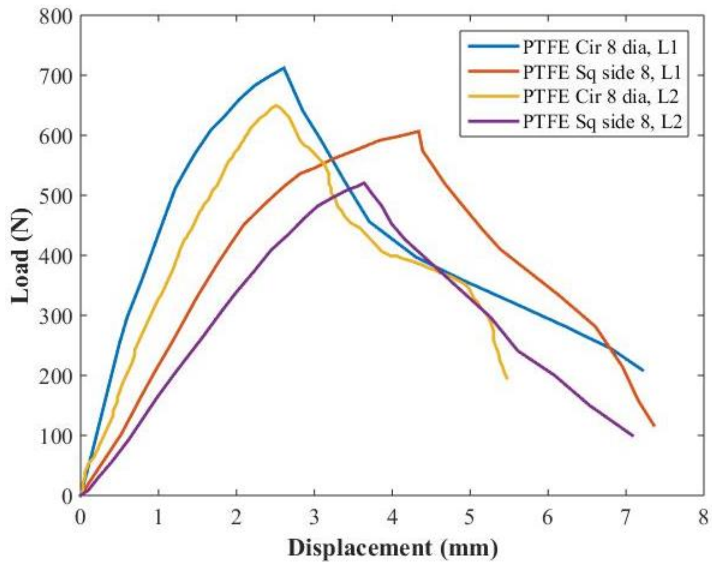
PTFE Cir 8 dia, L1
PTFE Sq side 8, L1
PTFE Cir 8 dia, L2
PTFE Sq side 8, L2
Load (N)
Displacement (mm)

(c)

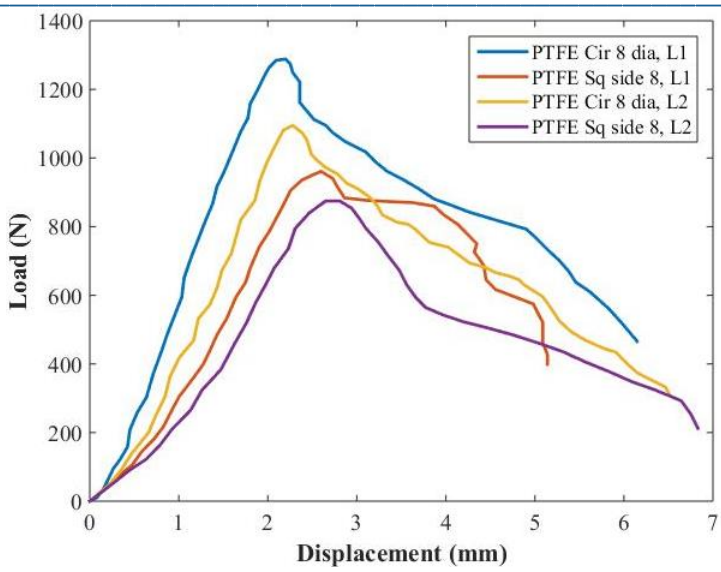

Fig. 5 - Flexural load-deflection curves of (a) E-glass/epoxy, (b) hybrid and (c) carbon/epoxy composites

4.2 Optimization of tensile and flexural strengths

HTLBO technique has been employed to optimize the distance of defect from top surface (*L*), area of defect (*A*) and density of laminate (*D*) for minimization of tensile and flexural strengths of delaminated E-glass/epoxy, carbon/epoxy and hybrid (E-glass/carbon/epoxy) composites. Mathematical models for tensile and flexural strengths were developed with experimental data using regression analysis.

Of this work, objective functions are to minimize σ_t (in MPa) = $4423 - 9.03L - 0.853A - 4376D + 1107.3D^2$ and σ_f (in MPa) = $18653 - 88.2L - 8.19A - 19530D + 5294D^2$ subject the parameter bounds 0.18 mm$<L<$0.9 mm, 50.256 mm^2$<A<$64 mm^2 and 1.4968 g/mm^3 $< D <$ 2.2116 g/mm^3.

Table 4 gives the initial population as per design of experiments, average values of input parameters and the ranks given based on the GRG values. The value of GRG for sample GE4 is minimum. Hence, first rank was given to it. The means of input parameters *L*, *A* and *D* were obtained to calculate new values of input parameters.

Table 4 - Initial population

Specimen	L	A	D	σ_t	σ_f	SNRA1	SNRA2	N-σ_t	N-σ_f	D-σ_t	D-σ_f	GRC-σ_t	GRC-σ_f	GRG	Rank
GE1	0.18	50.256	1.9314	52.45	201.76	-34.3949	-46.0967	0.085918716	0.199054	0.914081	0.800946	0.353586	0.384336	0.368961	4
GE2	0.9	50.256	1.9314	50.48	170.81	-34.0624	-44.6503	0.066123976	0.112064	0.933876	0.887936	0.348705	0.360247	0.354476	3
GE3	0.18	64	1.9314	47.38	149.88	-33.5119	-43.5149	0.033354136	0.043781	0.966646	0.956219	0.340914	0.343355	0.342134	2
GE4	0.9	64	1.9314	44.42	137.83	-32.9516	-42.7869	-1.72132E-06	-1.5E-06	1.000002	1.000001	0.333333	0.333333	0.333333	1

GCE1	0.18	50.256	2.116	84.39	592.78	-38.5258	-55.4579	0.331827434	0.762041	0.668173	0.237959	0.428019	0.677544	0.552782	8
GCE2	0.9	50.256	2.116	70.97	536.68	-37.0215	-54.5943	0.242276631	0.710106	0.757723	0.289894	0.397544	0.632996	0.51527	7
GCE3	0.18	64	2.116	63.98	507.38	-36.1209	-54.1067	0.188664183	0.680778	0.811336	0.319222	0.381291	0.610336	0.495813	6
GCE4	0.9	64	2.116	53.91	428.68	-34.6334	-52.6427	0.100114988	0.592732	0.899885	0.407268	0.357172	0.551105	0.454139	5
CE1	0.18	50.256	1.4968	307.26	934.82	-49.7501	-59.4146	0.999998245	0.999999	1.75E-06	1.21E-06	0.999996	0.999998	0.999997	12
CE2	0.9	50.256	1.4968	305.08	794.41	-49.6883	-58.0009	0.996316632	0.91498	0.003683	0.08502	0.992687	0.854672	0.923679	11
CE3	0.18	64	1.4968	299.51	697.44	-49.5282	-56.8701	0.98678913	0.846975	0.013211	0.153025	0.974258	0.765668	0.869963	10
CE4	0.9	64	1.4968	291.09	634.74	-49.2805	-56.0519	0.972044952	0.797767	0.027955	0.202233	0.94705	0.712015	0.829532	9
Mean	0.54	57.128	1.848201			-32.9516	-42.7869								

The difference of mean for *L*, *A* and *D* were calculated using the input variables for the first rank experiment. The selected random values for *L*, *A* and *D* are 0.91, 0.72 and 0.35 respectively [Ref 28]. Considering these random values, the difference of mean was calculated for the parameters associated with first rank.

Difference of mean for L = 0.91(0.9 – 0.54) = 0.3276 mm

Difference of mean for A = 0.72(64 – 57.128) =4.94784 mm^2

Difference of mean for D = 0.35(1.9314 – 1.848201) =0.02912 g/mm^3

The new process variables for *L*, *A* and *D* and their corresponding responses (σ_t and σ_f) are obtained as follows. The GRG values were also calculated using Eq. 7 and given in Table 5.

L_1 = 0.18 + 0.3276 = 0.5076 mm

A_1 = 50.256 + 4.94784 = 55.20384 mm^2

D_1 = 1.9314 + 0.02912 = 1.96052 g/mm^3

σ_t = 4423 - 9.03 × 0.5076 - 0.853 × 55.20384 – 4376 × 1.96052 + 1107.3 × 1.96052 × 1.96052 = 48.15 MPa

σ_f = 18653 – 88.2 × 0.5076 – 8.19 × 55.20384 – 19530 × 1.96052 + 5294 × 1.96054 × 1.96052 = 215.38 MPa

Table 5 - Updated input parameters, responses and GRG (teacher phase)

Specimen	L	A	D	σ_t	σ_f	SNRA-σ_t	SNRA-σ_f	N-σ_t	N-σ_f	D-σ_t	D-σ_f	GRC-σ_t	GRC-σ_f	GRG
GE1	0.5076	55.20384	1.96052	48.15	215.38	-33.6525	-46.664	0.134521117	0.277567	0.865479	0.722433	0.366172	0.40902	0.387596
GE2	0.9	55.20384	1.96052	44.61	180.77	-32.9886	-45.1424	0.09616331	0.182134	0.903837	0.817866	0.356167	0.379401	0.367784
GE3	0.5076	64	1.96052	40.65	143.34	-32.1812	-43.1272	0.049514944	0.055738	0.950485	0.944262	0.344712	0.346197	0.345455
GE4	0.9	64	1.96052	37.11	108.73	-31.389	-40.7268	0.00374502	-0.09481	0.996255	1.094814	0.334168	0.313516	0.323842
GCE1	0.5076	55.20384	2.145522	79.72	623.75	-38.0312	-55.9002	0.387507662	0.856858	0.612492	0.143142	0.449441	0.777434	0.613437
GCE2	0.9	55.20384	2.145522	76.17	589.14	-37.6362	-55.4044	0.364690365	0.82576	0.63531	0.17424	0.440408	0.741575	0.590992
GCE3	0.5076	64	2.145522	72.22	551.71	-37.1726	-54.8342	0.337900772	0.789999	0.662099	0.210001	0.430256	0.704224	0.56724
GCE4	0.9	64	2.145522	68.67	517.10	-36.7356	-54.2715	0.312652165	0.754705	0.687348	0.245295	0.421107	0.670875	0.545991
CE1	0.5076	55.20384	1.52592	272.17	681.61	-48.6969	-56.6707	1.003744981	0.905186	-0.00374	0.094814	1.007546	0.840599	0.924073
CE2	0.9	55.20384	1.52592	268.63	647.00	-48.5831	-56.2181	0.997168679	0.876797	0.002831	0.123203	0.994369	0.802307	0.898338
CE3	0.5076	64	1.52592	264.67	609.57	-48.4541	-55.7005	0.989716172	0.844332	0.010284	0.155668	0.979847	0.762581	0.871214
CE4	0.9	64	1.52592	261.13	574.96	-48.3371	-55.1928	0.982952178	0.812488	0.017048	0.187512	0.967029	0.72726	0.847144

The values of Table 4 and Table 5 are combined and the ranks are allotted on the basis of GRG in Table 6. The first rank was allotted to GE4 specimen and specimen CE1 secured last rank. This completes the teacher phase.

Table 6 - Combined population (teacher phase)

Specimen	L	A	D	σ_t	σ_f	SNRA1	SNRA2	N-σ_t	N-σ_f	D-σ_t	D-σ_f	GRC-σ_t	GRC-σ_f	GRG	Rank
GE1	0.18	50.256	1.9314	52.45	201.76	-34.3949	-46.0967	0.085918716	0.199054	0.914081	0.800946	0.353586	0.384336	0.368961	7
GE2	0.9	50.256	1.9314	50.48	170.81	-34.0624	-44.6503	0.066123976	0.112064	0.933876	0.887936	0.348705	0.360247	0.354476	5
GE3	0.18	64	1.9314	47.38	149.88	-33.5119	-43.5149	0.033354136	0.043781	0.966646	0.956219	0.340914	0.343355	0.342134	3
GE4	0.9	64	1.9314	44.42	137.83	-32.9516	-42.7869	-1.72132E-06	-1.5E-06	1.000002	1.000001	0.333333	0.333333	0.333333	2
GCE1	0.18	50.256	2.116	84.39	592.78	-38.5258	-55.4579	0.331827434	0.762041	0.668173	0.237959	0.428019	0.677544	0.552782	13
GCE2	0.9	50.256	2.116	70.97	536.68	-37.0215	-54.5943	0.242276631	0.710106	0.757723	0.289894	0.397544	0.632996	0.51527	11
GCE3	0.18	64	2.116	63.98	507.38	-36.1209	-54.1067	0.188664183	0.680778	0.811336	0.319222	0.381291	0.610336	0.495813	10
GCE4	0.9	64	2.116	53.91	428.68	-34.6334	-52.6427	0.100114988	0.592732	0.899885	0.407268	0.357172	0.551105	0.454139	9
CE1	0.18	50.256	1.4968	307.26	934.82	-49.7501	-59.4146	0.999998245	0.999999	1.75E-06	1.21E-06	0.999996	0.999998	0.999997	24
CE2	0.9	50.256	1.4968	305.08	794.41	-49.	-58.	0.996316632	0.91498	0.003683	0.08502	0.992687	0.854672	0.923679	22

						6883	0009								
CE3	0.18	64	1.4968	299.51	697.44	-49.5282	-56.8701	0.98678913	0.846975	0.013211	0.153025	0.974258	0.765668	0.869963	19
CE4	0.9	64	1.4968	291.09	634.74	-49.2805	-56.0519	0.972044952	0.797767	0.027955	0.202233	0.94705	0.712015	0.829532	17
GE1	0.5076	55.20384	1.96052	48.15308	215.378	-33.6525	-46.664	0.134521117	0.277567	0.865479	0.722433	0.366172	0.40902	0.387596	8
GE2	0.9	55.20384	1.96052	44.6097	180.768	-32.9886	-45.1424	0.09616331	0.182134	0.903837	0.817866	0.356167	0.379401	0.367784	6
GE3	0.5076	64	1.96052	40.64995	143.337	-32.1812	-43.1272	0.049514944	0.055738	0.950485	0.944262	0.344712	0.346197	0.345455	4
GE4	0.9	64	1.96052	37.10658	108.728	-31.389	-40.7268	0.00374502	-0.09481	0.996255	1.094814	0.334168	0.313516	0.323842	1
GCE1	0.5076	55.20384	2.145522	79.71822	623.749	-38.0312	-55.9002	0.387507662	0.856858	0.612492	0.143142	0.449441	0.777434	0.613437	16
GCE2	0.9	55.20384	2.145522	76.17485	589.139	-37.6362	-55.4044	0.364690365	0.82576	0.63531	0.17424	0.440408	0.741575	0.590992	15
GCE3	0.5076	64	2.145522	72.21509	551.708	-37.1726	-54.8342	0.337900772	0.789999	0.662099	0.210001	0.430256	0.704224	0.56724	14
GCE4	0.9	64	2.145522	68.67172	517.099	-36.7356	-54.2715	0.312652165	0.754705	0.687348	0.245295	0.421107	0.670875	0.545991	12
CE1	0.5076	55.20384	1.52592	272.1742	681.611	-48.	-56.	1.003744981	0.905186	-0.00374	0.094814	1.007546	0.840599	0.924073	23

						6969	6707								
CE2	0.9	55.20384	1.52592	268.6308	647.001	-48.5831	-56.2181	0.997168679	0.876797	0.002831	0.123203	0.994369	0.802307	0.898338	21
CE3	0.5076	64	1.52592	264.671	609.57	-48.4541	-55.7005	0.989716172	0.844332	0.010284	0.155668	0.979847	0.762581	0.871214	20
CE4	0.9	64	1.52592	261.1277	574.961	-48.3371	-55.1928	0.982952178	0.812488	0.017048	0.187512	0.967029	0.72726	0.847144	18

Nextly, based on the GRG rank of the teacher phase, the candidate solution was taken separately for delaminated E-glass/epoxy, carbon/epoxy and hybrid (E-glass/carbon/epoxy) composites from Table 6 and presented in Tables 7(a), 7(b) and 7(c) respectively.

Table 7(a) - Candidate solution based on the GRG for E-glass/epoxy composites (teacher phase)

Specimen	*L*	*A*	*D*	σ_t	σ_f	SNRA1	SNRA2	N-σ_t	N-σ_f	D-σ_t	D-σ_f	GRC-σ_t	GRC-σ_f	GRG	Rank
GE4	0.9	64	1.96052	37.10658	108.728	-31.389	-40.7268	0.00374502	-0.09481	0.996255	1.094814	0.334168	0.313516	0.323842	1
GE4	0.9	64	1.9314	44.42	137.83	-32.9516	-42.7869	-1.72132E-06	-1.5E-06	1.000002	1.000001	0.333333	0.333333	0.333333	2
GE3	0.18	64	1.9314	47.38	149.88	-33.5119	-43.5149	0.033354136	0.043781	0.966646	0.956219	0.340914	0.343355	0.342134	3
GE3	0.5076	64	1.96052	40.64995	143.337	-32.1812	-43.1272	0.049514944	0.055738	0.950485	0.944262	0.344712	0.346197	0.345455	4

Table 7(b) - Candidate solution based on the GRG for hybrid composites (teacher phase)

Specimen	*L*	*A*	*D*	σ_t	σ_f	SNRA1	SNRA2	N-σ_t	N-σ_f	D-σ_t	D-σ_f	GRC-σ_t	GRC-σ_f	GRG	Rank
GCE4	0.9	64	2.116	53.91	428.68	-34.6334	-52.6427	0.100114988	0.592732	0.899885	0.407268	0.357172	0.551105	0.454139	9

GCE3	0.18	64	2.116	63.98	507.38	-36.1209	-54.1067	0.188664183	0.680778	0.811336	0.319222	0.381291	0.610336	0.495813	10
GCE2	0.9	50.256	2.116	70.97	536.68	-37.0215	-54.5943	0.242276631	0.710106	0.757723	0.289894	0.397544	0.632996	0.51527	11
GCE4	0.9	64	2.145522	68.67172	517.099	-36.7356	-54.2715	0.312652165	0.754705	0.687348	0.245295	0.421107	0.670875	0.545991	12

Table 7(c) - Candidate solution based on the GRG for carbon/epoxy composites (teacher phase)

Specimen	L	A	D	σ_t	σ_f	SNRA1	SNRA2	N-σ_t	N-σ_f	D-σ_t	D-σ_f	GRC-σ_t	GRC-σ_f	GRG	Rank
CE4	0.9	64	1.4968	291.09	634.74	-49.2805	-56.0519	0.972044952	0.797767	0.027955	0.202233	0.94705	0.712015	0.829532	17
CE4	0.9	64	1.52592	261.1277	574.961	-48.3371	-55.1928	0.982952178	0.812488	0.017048	0.187512	0.967029	0.72726	0.847144	18
CE3	0.18	64	1.4968	299.51	697.44	-49.5282	-56.8701	0.98678913	0.846975	0.013211	0.153025	0.974258	0.765668	0.869963	19
CE3	0.50776	64	1.52592	264.671	609.57	-48.4541	-55.7005	0.989716172	0.844332	0.010284	0.155668	0.979847	0.762581	0.871214	20

The knowledge was transferred among the learners through interaction. The interaction took place between the fast learner and slow learner. The slow learner acquires knowledge to enhance his/her academic performance. In the present case, the transfer of knowledge took place between the topper (1^{st} rank specimen) and the slow learner (4^{th} rank specimen) as shown in Table 8(a). The selected random values for L, A and D are 0.81, 0.79 and 0.45 respectively. The new values of L, A and D for E-glass/epoxy composites are obtained as follows.

New L = 0.9+ 0.81(0.9 – 0.5076) = 1.2178 mm

New A = 64 + 0.79(64 – 64) = 64 mm^2

New D = 1.96052 + 0.35(1.96052 – 1.96052) = 1.96052 g/mm^3

The interaction took place between 2^{nd} and 3^{rd}, 3^{rd} and $4^{th}$and also 4^{th} and 1^{st} rank specimens. The obtained input variables were substituted in the objective functions to get the responses and are given in Table 8(a).

Table 8(a) - New values of L, A, D, σ_t, σ_f and GRG for E-glass/epoxy composites (learner phase)

Specimen	L	A	D	σ_t	σ_f	SNRA1	SNRA2	N-σ_t	N-σ_f	D-σ_t	D-σ_f	GRC-σ_t	GRC-σ_f	GRG	Interaction
GE4	0.9	64	1.96	42.106	108.09	-31.3933	-40.6757	-2.213	6.58547E-07	1.000022	0.999999	0.333328	0.333333	0.333331	1 and 4

								77E-05							
GE4	0.9	64	1.93	43.18	76.18	-31.8619	-37.6369	0.22738509	-2.64884E-12	0.772615	1	0.392892	0.333333	0.363113	2 and 3
GE3	0.18	64	1.918	47.07	129.59	-33.4541	-42.2514	0.999978025	9.99997E-07	2.2E-05	0.999999	0.999956	0.333334	0.666645	3 and 4
GE3	0.825	64	1.96	37.80	114.71	-31.5503	-41.1917	0.076172825	7.70355E-07	0.923827	0.999999	0.351166	0.333334	0.34225	4 and 1

The transfer of knowledge took place between the topper (9th rank specimen) and the slow learner (12th rank specimen) as shown in Table 7(b). The corresponding preferred random values for *L*, *A* and *D* were taken as 0.81, 0.79 and 0.45. The new values of *L*, A and *D* for hybrid composites are obtained as follows.

New L = 0.9 + 0.81 (0.9 – 0.9) = 0.9 mm

New A = 64 + 0.79 (64 – 64) = 64 mm^2

New D = 2.116402 + 0.35 (2.116402 – 2.145522) = 2.103298 g/mm^3

In the same manner the interaction took place between 10thand 11th, 11thand 12th and also 12thand 9th rank specimens. The obtained input variables were substituted in the objective functions to get the responses and are tabulated in Table 8(b).

Table 8(b) - New values of *L, A, D,* σ_t, σ_f and GRG for hybrid composites (learner phase)

Specimen	L	A	D	σ_t	σ_f	SNRA1	SNRA2	N-σ_t	N-σ_f	D-σ_t	D-σ_f	GRC-σ_t	GRC-σ_f	GRG	Interaction
GCE4	0.9	64	2.103298	56.22	898.91	-34.7743	-59.0743	1.66473E-05	5.08042E-05	0.999983	0.999949	0.333337	0.333345	0.333341	9 and 12
GCE3	0.18	74.85	2.116	57.92	999.12	-34.9519	-59.9923	0.105400718	1.000050562	0.894599	-5.1E-05	0.358526	1.000101	0.679314	10 and 11
GCE2	0.9	50.25	2.103298	66.52	898.91	-36.4591	-59.0743	1.000016841	5.08042E-05	-1.7E-05	0.999949	1.000034	0.333345	0.666689	11 and 12
GCE1	0.9	64	2.132418	63.94	982.94	-36.1157	-59.8506	0.796163604	0.845611858	0.203836	0.154388	0.710392	0.764073	0.737232	12 and 9

The transfer of knowledge took place between the topper (1strank specimen) and the slow learner (3rdrank specimen) as shown in Table 8(c). The random numbers were taken as 0.81, 0.79 and 0.45 correspondingly. The new values of *L*, *A* and *D* for carbon/epoxy composites are obtained as follows.

New L = 0.9 + 0.81 (0.9 – 0.5076) = 0.9 mm

New A = 64+ 0.79 (64 – 64) = 64 mm^2

New D = 1.4968 + 0.35 (1.4968 – 1.4968) = 1.4968 g/mm^3

Likewise, the interaction took place between 18th and 19th, 19th and 20th, and also 20th and 17th rank specimens. The obtained input variables were substituted in the objective function to get the responses and are tabulated in Table 8(c).

Table 8(c) - New values of *L, A, D*, σ_t, σ_f and GRG for carbon/epoxy composites (learner phase)

Specimen	L	A	D	σ_t	σ_f	SNRA1	SNRA2	N-σ_t	N-σ_f	D-σ_t	D
CE4	0.9	64	1.4968	291.09	677.69	-49.2806	-56.6206	0.878098688	0.730283813	0.121901312	0
CE4	0.9	64	1.539	248.28	631.74	-47.8988	-54.514	2.88164E-05	-3.65148E-06	0.999971184	1
CE3	0.18	64	1.4968	297.59	741.19	-49.4724	-57.3986	1.000029079	0.999996271	-2.9079E-05	3
CE3	0.825	64	1.5128	275.28	626.75	-48.7889	-55.9419	0.565673901	0.494989711	0.434326099	0

After the transfer of knowledge among the learners, the performance of learner enhances and to observe this difference, the population was combined. The combined population of delaminated composites is given in Table 9 (a-c).

Table 9(a) - Combined population for E-glass/epoxy composites (learner phase)

Specimen	L	A	D	σ_t	σ_f	SNRA1	SNRA2	N-σ_t	N-σ_f	D-σ_t	D-σ_f	GRC-σ_t	GRC-σ_f	GRG
GE4	0.9	64	1.96052	42.10	128.7275	-31.389	-40.7268	0.00374502	-0.094814097	0.996255	1.094814	0.334168	0.313516	0.323842
GE4	0.9	64	1.9314	44.42	137.83	-32.9516	-42.7869	-1.72132E-06	-1.49612E-06	1.000002	1.000001	0.333333	0.333333	0.333333
GE3	0.18	64	1.9314	47.38	149.88	-33.5119	-43.5149	0.033354136	0.043780833	0.966646	0.956219	0.340914	0.343355	0.342134
GE3	0.5076	64	1.96052	40.65	143.3372	-32.1812	-43.1272	0.049514944	0.055737691	0.950485	0.944262	0.344712	0.346197	0.345455
GE4	0.9	64	1.96	37.12	108.09	-31.3933	-40.6757	-2.21377E-05	6.58547E-07	1.000022	0.999999	0.333328	0.333333	0.333331
GE4	0.9	64	1.93	39.18	76.18	-31.8619	-37.6369	0.22738509	-2.64884E-12	0.772615	1	0.392892	0.333333	0.363113
GE3	0.18	64	1.918	47.07	129.59	-33.4541	-42.2514	0.999978025	9.99997E-07	2.2E-05	0.999999	0.999956	0.333334	0.666645

GE3	0.825	64	1.96	37.80	114.71	-31.5503	-41.1917	0.076172825	7.7035E-07	0.923827	0.999999	0.351166	0.333334	0.34225

Table 9(b) - Combined population for hybrid composites (learner phase)

TYPE	L	A	D	σ_t	σ_f	SNRA1	SNRA2	N-σ_t	N-σ_f	D-σ_t	D-σ_f	GRC-σ_t	GRC-σ_f	GRG
GCE4	0.9	64	2.116	53.91	428.68	-34.6334	-52.6427	0.100114988	0.592732386	0.899885	0.407268	0.357172	0.551105	0.454139
GCE3	0.18	64	2.116	63.98	507.38	-36.1209	-54.1067	0.188664183	0.68077849	0.811336	0.319222	0.381291	0.610336	0.495813
GCE4	0.9	50.256	2.116	70.97	536.68	-37.0215	-54.5943	0.242276631	0.710105572	0.757723	0.289894	0.397544	0.632996	0.51527
GCE4	0.9	64	2.145522	68.6717	517.09878	-36.7356	-54.2715	0.312652165	0.754704939	0.687348	0.245295	0.421107	0.670875	0.545991
GCE4	0.9	64	2.103298	56.22	438.91	-34.7743	-59.0743	1.66473E-05	5.08042E-05	0.999983	0.999949	0.333337	0.333345	0.333341
GCE3	0.18	74.85	2.116	55.92	999.12	-34.9519	-59.9923	0.105400718	1.000050562	0.894599	-5.1E-05	0.358526	1.000101	0.679314
GCE2	0.9	50.25	2.103298	66.52	898.91	-36.4591	-59.0743	1.000016841	5.08042E-05	-1.7E-05	0.999949	1.000034	0.333345	0.666689
GCE1	0.9	64	2.132418	63.94	982.94	-36.1157	-59.8506	0.796163604	0.845611858	0.203836	0.154388	0.710392	0.764073	0.737232

Table 9(c) Combined population for carbon/epoxy composites (learner phase)

Specimen	L	A	D	σ_t	σ_f	SNRA1	SNRA2	N-σ_t	N-σ_f	D-σ_t	D-σ_f	GRC-σ_t	GRC-σ_f	GRG
CE4	0.9	64	1.4968	291.09	634.74	-49.2805	-56.0519	0.972044952	0.797767178	0.027955048	0.202233	0.94705	0.712015	0.829532
CE4	0.9	64	1.52592	261.1277	574.960595	-48.3371	-55.1928	0.982952178	0.812488107	0.017047822	0.187512	0.967029	0.72726	0.847144

CE3	0.18	64	1.4968	299.51	697.44	-49.5282	-56.8701	0.98678913	0.846975467	0.01321087	0.153025	0.974258	0.765668	0.869963
CE3	0.5076	64	1.52592	264.671	609.570275	-48.4541	-55.7005	0.989716172	0.844331804	0.010283828	0.155668	0.979847	0.762581	0.871214
CE4	0.9	64	1.4968	291.09	677.69	-49.2806	-56.6206	0.878098688	0.730283813	0.121901312	0.269716	0.803986	0.64959	0.726788
CE4	0.9	64	1.539	275.28	631.74	-47.8988	-54.514	2.88164E-05	-3.65148E-06	0.999971184	1.000004	0.33334	0.333333	0.333336
CE3	0.18	64	1.4968	297.59	741.19	-49.4724	-57.3986	1.000029079	0.999996271	-2.9079E-05	3.73E-06	1.000058	0.999993	1.000025
CE3	0.825	64	1.5128	275.07	626.75	-48.7889	-55.9419	0.565673901	0.494989711	0.434326099	0.50501	0.535145	0.497507	0.516326

Based on the GRG value the ranks were allotted for E-glass/epoxy, hybrid and carbon/epoxy composites and are presented in the Table 10 (a-c).

Table 10 (a) - Order of preference in samples for minimization of tensile and flexural strengths of E-glass/epoxy composites

Specimen	L	A	D	σ_t	σ_f	SNRA1	SNRA2	N-σ_t	N-σ_f	D-σ_t	D-σ_f	GRC-σ_t	GRC-σ_f	GRG	Rank
GE4	0.9	64	1.96052	42.10	128.7275	-31.389	-40.7268	0.00374502	-0.094814097	0.996255	1.094814	0.334168	0.313516	0.323842	1
GE4	0.9	64	1.9314	44.42	137.83	-32.9516	-42.7869	-1.72132E-06	-1.49612E-06	1.000002	1.000001	0.333333	0.333333	0.333333	3
GE3	0.18	64	1.9314	47.38	149.88	-33.5119	-43.5149	0.033354136	0.043780833	0.966646	0.956219	0.340914	0.343355	0.342134	4
GE3	0.5076	64	1.96052	40.65	143.3372	-32.1812	-43.1272	0.049514944	0.055737691	0.950485	0.944262	0.344712	0.346197	0.345455	6
GE4	0.9	64	1.96	37.12	108.09	-31.3933	-40.6757	-2.21377E-05	6.58547E-07	1.000022	0.999999	0.333328	0.333333	0.333331	2

GE4	0.9	64	1.93	39.18	76.18	-31.8619	-37.6369	0.22738509	-2.64884E-12	0.772615	1	0.392892	0.333333	0.363113	7
GE3	0.18	64	1.918	47.07	129.59	-33.4541	-42.2514	0.999978025	9.99997E-07	2.2E-05	0.999999	0.999956	0.333334	0.666645	8
GE3	0.825	64	1.96	37.80	114.71	-31.5503	-41.1917	0.076172825	7.70355E-07	0.923827	0.999999	0.351166	0.333334	0.34225	5

Table 10 (b) - Order of preference in samples for minimization of tensile and flexural strengths of hybrid composites

Specimen	L	A	D	σ_t	σ_f	SNRA1	SNRA2	N-σ_t	N-σ_f	D-σ_t	D-σ_f	GRC-σ_t	GRC-σ_f	GRG	Rank
GCE4	0.9	64	2.116	53.91	428.68	-34.6334	-52.6427	0.100114988	0.592732386	0.899885	0.407268	0.357172	0.551105	0.454139	2
GCE3	0.18	64	2.116	63.98	507.38	-36.1209	-54.1067	0.188664183	0.68077849	0.811336	0.319222	0.381291	0.610336	0.495813	3
GCE2	0.9	50.256	2.116	70.97	536.68	-37.0215	-54.5943	0.242276631	0.710105572	0.757723	0.289894	0.397544	0.632996	0.51527	4
GCE4	0.9	64	2.145522	68.6717	517.09878	-36.7356	-54.2715	0.312652165	0.754704939	0.687348	0.245295	0.421107	0.670875	0.545991	5
GCE4	0.9	64	2.103298	56.22	438.91	-34.7743	-59.0743	1.66473E-05	5.08042E-05	0.999983	0.999949	0.333337	0.333345	0.333341	1
GCE3	0.18	74.85	2.116	55.92	999.12	-34.9519	-59.9923	0.105400718	1.000050562	0.894599	-5.1E-05	0.358526	1.000101	0.679314	7

GCE2	0.9	50.25	2.103298	66.52	898.91	-36.4591	-59.0743	1.000016841	5.08042E-05	-1.7E-05	0.999949	1.000034	0.333345	0.666689	6
GCE1	0.9	64	2.132418	63.94	982.94	-36.1157	-59.8506	0.796163604	0.845611858	0.203836	0.154388	0.710392	0.764073	0.737232	8

Table 10 (c) - Order of preference in samples for minimization of tensile and flexural strengths of carbon/epoxy composites

Specimen	L	A	D	σ_t	σ_f	SNRA1	SNRA2	N-σ_t	N-σ_f	D-σ_t	D-σ_f	GRC-σ_t	GRC-σ_f	GRG	Rank
CE4	0.9	64	1.4968	291.09	634.74	-49.2805	-56.0519	0.972044952	0.797767178	0.027955048	0.202233	0.94705	0.712015	0.829532	4
CE4	0.9	64	1.52592	261.1277	574.960595	-48.3371	-55.1928	0.982952178	0.812488107	0.017047822	0.187512	0.967029	0.72726	0.847144	5
CE3	0.18	64	1.4968	299.51	697.44	-49.5282	-56.8701	0.98678913	0.846975467	0.01321087	0.153025	0.974258	0.765668	0.869963	6
CE3	0.5076	64	1.52592	264.671	609.570275	-48.4541	-55.7005	0.989716172	0.844331804	0.010283828	0.155668	0.979847	0.762581	0.871214	7
CE4	0.9	64	1.4968	291.09	677.69	-49.2806	-56.6206	0.878098688	0.730283813	0.121901312	0.269716	0.803986	0.64959	0.726788	3
CE4	0.9	64	1.539	275.28	631.74	-47.8988	-54.514	2.88164E-05	-3.65148E-06	0.999971184	1.000004	0.33334	0.333333	0.333336	1
CE3	0.18	64	1.4968	297.59	741.19	-49.4724	-57.3986	1.000029079	0.999996271	-2.9079E-05	3.73E-06	1.000058	0.999993	1.000025	8
CE3	0.825	64	1.5128	275.07	626.75	-48.	-55.	0.565673901	0.494989711	0.434326099	0.50501	0.535145	0.497507	0.516326	2

7889	9419

Table 11 - Final solution

Specimen	*L*	*A*	*D*	σ_t	σ_f	SNRA1	SNRA2	N-σ_t	N-σ_f	D-σ_t	D-σ_f	GRC-σ_t	GRC-σ_f	GRG
GE4	0.9	64	1.96052	42.10658	128.72752	-31.389	-40.7268	0.00374502	-0.094814097	0.99625498	1.094814	0.334168	0.313516	0.323842
GCE4	0.9	64	2.103298	56.22	438.91	-34.7743	-59.0743	1.66473E-05	5.08042E-05	0.999983353	0.999949	0.333337	0.333345	0.333341
CE4	0.9	64	1.539	275.28	631.74	-47.8988	-54.514	2.88164E-05	-3.65148E-06	0.999971184	1.000004	0.33334	0.333333	0.333336

Table 11 gives the final solution for minimization of tensile and flexural strengths of E glass/epoxy, carbon/epoxy and hybrid composites. The input variables identified in table 11 are identified as optimal variables for minimization of tensile and flexural strengths. It has been observed that the tensile and flexural strengths are minimum when the composite contains square defect at the interface between 5^{th} and 6^{th} plies.

Table 12 Validation of HTLBO results with experimental values

Specimen	*L*	*A*	*D*	σ_t-Experiment	σ_t-HTLBO	σ_f-Experiment	σ_f-HTLBO
GE4	0.9	64	1.96052	44.4292	42.10658	137.33	128.72752
GCE4	0.9	64	2.103298	53.913	56.22	428.68	438.91
CE4	0.9	64	1.539	291.095	275.28	634.74	631.74

Table 12 shows the comparison of HTLBO results with experimental values. The HTLBO results agreed with experimental values within 4% error. From the optimal solutions it is clear that the composite containing a square defect at the interface between 5^{th} and 6^{th} layers possesses minimum tensile and flexural strengths.

5. Conclusions

In the present study, static tensile and three-point bending tests were conducted on multilayered E-glass/epoxy, carbon/epoxy and hybrid composite laminates containing single artificial defect with variable shape at the selected ply interface to study their behaviors due to induced delamination. Additionally, a hybrid TLBO was implemented to optimize the process variables for minimization of tensile and flexural strengths. Based on the results obtained, the following conclusions may be drawn from the present work are presented hereunder.

- The location of artificial defect with same shape and size in E-glass/epoxy and carbon/epoxy composites did not affect the tensile strengths.
- The location of PTFE in hybrid composite with same shape and size affected the tensile strength due to higher stiffness and strength of carbon fibre.
- The location of induced delamination affected stiffnesses of all composites regardless of shape and size due to destruction of structural integrity.

- The flexural properties decreased for the laminates containing circular or square artificial defect existing at different depths with respect to outer surface.
- HTLBO suggests that the composite containing square defect at the interface between 5th and 6th plies possesses minimum tensile and flexural strengths.

References

[1] Egbo, M. K. (2021). A fundamental review on composite materials and some of their applications in biomedical engineering. Journal of King Saud University – Engineering Sciences, 33(8), 557-568.
[2] Diamanti, K. & Soutis, C. (2010). Structural health monitoring techniques for aircraft composite structures. Progress in Aerospace Sciences, 46(8), 342-352.
[3] Szebenyi, G. & Hliva, V. (2019). Detection of delamination in polymer composites by digital image correlation-experimental test. Polymers, 11(3), 523.
[4] Aslan, Z. & Daricik, F. (2016). Effects of multiple delaminations on the compressive, tensile, flexural, and buckling behaviour of E-glass/epoxy composites. Composites Part B: Engineering, 100, 186-196.
[5] Reis, P. N. B., Ferreira, J. A. M., Antunes, F. V. & Richardson, M. O. W. (2009). Effect of interlayer delamination on mechanical behaviour of carbon/epoxy laminates. Journal of Composites Materials, 43(22), 2609-2621.
[6] Ashir, M., Nocke, A. & Cherif, C. (2019). Effect of the position of defined local defect on the mechanical performance of carbon-fiber-reinforced plastics. Autex Research Journal, 19(1), 74-79.
[7] Amaro, A. M., Reis, P. N. B. & De Moura, M. F. S. F. (2011). Delamination effect on bending behaviour in carbon–epoxy composites. Strain, 47(2), 203-208.
[8] Liu, Z., Li, P. & Srikanth, N. (2019). Effect of delamination on the flexural response of $[+45/-45/0]_{2s}$ carbon fibre reinforced polymer laminates. Composites Structures, 209, 93-102.
[9] Pradeep, D., Janardhana Reddy, N., Rahul Kumar, C., Srikanth, L. & Rao, R. M. V. G. K. (2007). Studies on mechanical behaviour of glass epoxy composites with induced defects and correlations with NDT characterization parameters. Journal of Reinforced Plastics and Composites, 26(15), 1539-1556.
[10] Kopparthi, P. K., Aerra, K. K. Y., Pathakokila, B. R., Gamini, S. (2020). Bending and viscoelastic behaviour of delaminated woven E-glass/epoxy composite. Australian Journal of Mechanical Engineering, 20(5): 1300-1309.
[11] Kopparthi, P. K., Gemaraju, S., Pathakokila, B. R. & Gamini, S. (2021). Experimental investigations on flexural behaviour of delaminated carbon/epoxy composite using three-dimensional digital image correlation. Proceedings of the Institution of Mechanical Engineers, Part C: Journal of Mechanical Engineering Science, 235(12), 2265-2275.
[12] Kopparthi, P. K., Kundavarapu, V. R., Dasari, V. R., Kaki, V. R. & Pathakokila, B. R. (2020). Modeling of glass fiber reinforced composites for optimal mechanical properties using teaching learning-based optimization and artificial neural networks. SN Applied Sciences, 2(1), 1-15.
[13] Das, B., Roy, S., Rai, R. N. & Saha, S. C. (2018). Multiobjective optimization of in situ process parameters in preparation of Al-4.5% Cu-TiC MMC using a grey relation-based teaching–learning-based optimization algorithm. Proceedings of the Institution of Mechanical Engineers, Part E: Journal of Process Mechanical Engineering, 232(4), 393-407.
[14] Rudrapati, R., Rathod, L., Patil, A. G., Santosh, C. & Dega, N. (2016). Parametric optimization for turning of GFRP composites using elitist teaching learning-based optimization (ETLBO). International Journal of Advances in Production and Mechanical Engineering, 2, 25-30.
[15] Abhishek, K., Kumar, V. R., Datta, S. & Mahapatra, S. S. (2017). Parametric appraisal and optimization in machining of CFRP composites by using TLBO (teaching-learning based optimization algorithm). Journal of Intelligent Manufacturing, 28(8), 1769-1785.
[16] Abhishek, K., Datta, S. & Mahapatra, S. S. (2017). Optimization of MRR, surface roughness, and maximum tool-tip temperature during machining of CFRP composites. Materials today: proceedings, 4(2), 2761-2770.
[17] Chen, Y. K., Weng. S. X. & Liu, T. P. (2020) Teaching-Learning Based Optimization (TLBO) with Variable Neighborhood Search to Retail Shelf-Space Allocation. Mathematics, 8(8), 1296.

[18] Cui, Z., Li, C., Dai, W., Zhang, L. & Wu, Y. (2020). A hierarchical teaching-learning-based optimization algorithm for optimal design of hybrid active power filter. IEEE Access, 8, 143530-143544.

[19] Halleh, H., Sadati, A. & Hajisharifi, N. (2020). Operation Sequencing Optimization in CAPP Using Hybrid Teaching-Learning Based Optimization (HTLBO). Journal of Optimization in Industrial Engineering, 13(1): 123-130.

[20] Nadeem, Z., Javaid, N., Malik, A. W. & Iqbal, S. (2018). Scheduling appliances with GA, TLBO, FA, OSR and their hybrids using chance constrained optimization for smart homes. Energies, 11(4), 888.

[21] Navaneethakrishnan, S. & Athijayamani, A. (2015). Taguchi method for optimization of fabrication parameters with mechanical properties in fiber and particulate reinforced composites. International Journal of Plastics Technology, 19(2), 227-240.

[22] Sharma, N., Ahuja, N., Goyal, R. & Rohilla, V. (2020). Parametric optimization of EDD using RSM-Grey-TLBO-based MCDM approach for commercially pure titanium. Grey Systems: Theoritical & Applications, 10(2), 231-245.

[23] Hong, Q. & Shi. Y. (2020). Multi response Parameter Optimization for the Composite Tape Winding Process Based on GRA and RSM. Mathematical Problems in Engineering, 1-8.

[24] Gangil, B., Ranakoti, L., Verma, S., Singh, T. & Kumar, S. (2020). Natural and Synthetic Fibers for Hybrid Composites. Hybrid Fiber Composites: Materials, Manufacturing Process Engineering, 1-15.

[25] Puttegowda, M., Thyavihalli Girijappa, Y. G., Mavinkere Rangappa, S., Parameswaranpillai, J. & Siengchin, S. (2020). Effect of process engineering on the performance of hybrid fiber composites. Hybrid Fiber Composites: Materials, Manufacturing Process Engineering, 17-40.

[26] ASTM Standard D3039. (1999). Standard Test Method for Tensile Properties of Polymer Matrix Composite Material, American Society for Testing and Materials, West Conshohocken, PA.

[27] ASTM D790-03. (2003). Standard Test Methods for Flexural Properties of Unreinforced and Reinforced Plastics and Electrical Insulating Materials. ASTM International, West Conshohocken, PA. doi: 10.1520/D0790-03.

[28] Kopparthi, P. K., Kundavarapu, V. R., Kaki, V. R. & Pathakokila, B. R. (2021). Modeling and multi response optimization of mechanical properties for E-glass/polyester composite using Taguchi-grey relational analysis. Proceedings of the Institution of Mechanical Engineers, Part E: Journal of Process Mechanical Engineering, 235(2), 342-350.